Quantum Quadrature Amplitude Modulation with Photon-Added Gaussian States

Andrea Giani*, Moe Z. Win†, and Andrea Conti*

*Department of Engineering and CNIT, University of Ferrara, Via Saragat 1, 44122 Ferrara, Italy
(e-mail: andrea.giani@unife.it, a.conti@ieee.org)

†Laboratory for Information and Decision Systems, Massachusetts Institute of Technology, Cambridge, MA 02139 USA
(e-mail: moewin@mit.edu)

GLOBECOM 2023 - 2023 IEEE Global Communications Conference | 979-8-3503-1090-0/23/$31.00 ©2023 IEEE | DOI: 10.1109/GLOBECOM54140.2023.10437870

***Abstract*—Quantum communication systems exchange information between a source and a destination by encoding such information into quantum states according to modulation techniques. The design of quantum modulation techniques, including quantum quadrature amplitude modulation (QAM), requires choosing and characterizing quantum states. This paper explores the use of non-Gaussian photon-added Gaussian states (PAGSs) for quantum QAM communications. First, we characterize pure PAGSs in the Fock space and derive a closed-form expression for their inner product. Then, we develop a quantum QAM technique employing PAGSs. In particular, we show how to construct quantum QAM constellations of PAGSs. Finally, we evaluate the performance of the developed quantum QAM technique with PAGSs, when a square root measurement (SRM) receiver is employed, and compare such performance with that of existing coherent states. Results show that PAGSs can provide a performance gain with respect to coherent states.**

***Index Terms*—Quantum communications, quantum constellation, photon-added Gaussian state, quantum receiver.**

I. Introduction

Quantum communications is a promising area of quantum information theory that relies on the exploitation of quantum mechanical laws to convey information through a quantum channel [1]–[7]. In a quantum communication system, classical information is encoded into the variation of physical characteristics of quantum states according to a modulation technique, thus determining the quantum constellation. The states of the quantum constellation are then used to convey information to the destination. Information carried by the quantum states is retrieved by employing a quantum receiver that discriminates which states were transmitted [8]–[13]. Therefore, the communication performance, in terms of symbol error probability (SEP), is related to the discrimination error probability. Determining the SEP is a hard task since it depends on the adopted modulation technique, states of the constellation, decoherence effects introduced by a noisy quantum channel, and the employed quantum receiver.

In the literature, quantum pulse position modulation (PPM) [7], [13]–[16] and phase shift keying (PSK) [7], [17]–[21] techniques have been studied for constellations of arbitrary Gaussian states, while quadrature amplitude modulation (QAM) only for constellations of coherent states [7], [20]–[23]. Recently, it has been shown for PPM that constellations of non-Gaussian states can provide better performance than Gaussian states [24], [25]. Both PPM and PSK constellations are shown to exhibit geometrically uniform symmetry (GUS), while QAM constellations generally do not. Optimal quantum receivers, that can achieve the minimum error probability, are known only for constellations that exhibit either a high mean number of photons [9] or GUS [16], [26]–[29]. Constellations without GUS require to employ sub-optimal receivers that do not achieve the minimum error probability. Except for PPM, quantum modulation techniques with constellations of non-Gaussian states have not been explored yet.

This paper explores the use of pure non-Gaussian photon-added Gaussian states (PAGSs) for quantum QAM communications. The key contributions of this paper can be summarized as follows: (i) we derive the Fock representation and the inner product of pure PAGSs; (ii) we develop the quantum QAM technique employing PAGSs; and (iii) we evaluate the SEP of quantum QAM communications with PAGSs.

The remaining sections are organized as follows: Section II introduces the quantum QAM technique and provides some useful results on Hermite polynomials. Section III derives the Fock representation and the inner product of pure PAGSs. Section IV develops quantum QAM employing PAGSs. Section V evaluates the SEP of the quantum QAM with PAGSs, when a square root measurement (SRM) receiver is employed, and compares such SEP with that of existing coherent states. Finally, Section VI gives our conclusions.

Notations: Random variables are displayed in sans serif, upright fonts; their realizations in serif, italic fonts. Operators are denoted by uppercase letters. For example, a random variable and its realization are denoted by x and x, respectively; an operator is denoted by $\boldsymbol{X}$. The sets of complex numbers and of natural numbers are denoted by $\mathbb{C}$ and $\mathbb{N}$, respectively. For a set $\mathcal{A}$: $|\mathcal{A}|$ denotes the cardinality, i.e., the number of elements, of $\mathcal{A}$. For $z \in \mathbb{C}$: $|z|$ denotes the absolute value; z^* denotes the complex conjugate; and $\imath = \sqrt{-1}$. The adjoint of an operator is denoted by $(\cdot)^\dagger$. The annihilation and the creation operators are denoted by $\boldsymbol{A}$ and $\boldsymbol{A}^\dagger$, respectively. The identity operator defined on a Hilbert space $\mathcal{H}$ is denoted by $\boldsymbol{I}_{\mathcal{H}}$. For two operators $\boldsymbol{X}$ and $\boldsymbol{Y}$, the commutator is denoted by $[\![\boldsymbol{X},\boldsymbol{Y}]\!]_- = \boldsymbol{XY} - \boldsymbol{YX}$. The displacement operator with parameter $\mu \in \mathbb{C}$ is $\boldsymbol{D}_\mu = \exp\{\mu \boldsymbol{A}^\dagger - \mu^* \boldsymbol{A}\}$. The rotation operator with parameter $\phi \in \mathbb{R}$ is $\boldsymbol{R}_\phi = \exp\{\imath\phi \boldsymbol{A}^\dagger \boldsymbol{A}\}$. The squeezing operator with parameter $\zeta \in \mathbb{C}$ is $\boldsymbol{S}_\zeta = \exp\{\frac{1}{2}\zeta(\boldsymbol{A}^\dagger)^2 - \frac{1}{2}\zeta^* \boldsymbol{A}^2\}$. The squeezing parameter $\zeta \in \mathbb{C}$ can equivalently be written as $\zeta = re^{\imath\theta}$, with $r \geqslant 0$ and $-\pi < \theta \leqslant \pi$.

II. Preliminaries

This section introduces the quantum QAM technique and presents some known results on Hermite polynomials that are used in the rest of the paper.

A. Quantum Quadrature Amplitude Modulation

In a quantum communication system, classical information is encoded into the variation of suitable characteristics of quantum states. Such states are then used for conveying the information to a destination. In QAM systems, classical information is represented with symbols in the alphabet

$$\mathcal{A}_M^{(\Delta)} = \{a_{i,j} = \Delta(p_i + \imath\, q_j),\, p_i, q_j \in \mathcal{A}_L\} \tag{1}$$

where $\mathcal{A}_L = \{a_k = 2k - L - 1, k = 1, 2, \dots, L\}$ and $L = 2^n$, with $n \geqslant 1$ integer. Symbols $a_{i,j}$ have prior probabilities $\mathbb{P}\{\mathsf{a} = a_{i,j}\}$ such that $\sum_{i,j=1}^{L} \mathbb{P}\{\mathsf{a} = a_{i,j}\} = 1$. In (1), $|\mathcal{A}_M^{(\Delta)}| = M = L^2$, and Δ is related to the constellation energy and represents the spacing of the symbols in the complex plane. The constellation of a quantum M-QAM system is

$$\mathcal{C}_M^{(\Delta)} = \left\{|\psi_{i,j}\rangle \in \mathcal{H} : |\psi_{i,j}\rangle = |\psi(a_{i,j})\rangle\,, a_{i,j} \in \mathcal{A}_M^{(\Delta)}\right\} \tag{2}$$

where $\mathcal{H}$ is the Hilbert space associated with the quantum communication system. In (2), $\mathcal{C}_M^{(\Delta)}$ is obtained by mapping each classical symbol $a_{i,j} \in \mathcal{A}_M^{(\Delta)}$ to the corresponding quantum state $|\psi_{i,j}\rangle$. Specifically, $|\psi_{i,j}\rangle$ is obtained by varying suitable characteristics of an initial state $|\psi\rangle$ by a quantity that depends on $a_{i,j}$. Notice that the geometrical structure of $\mathcal{A}_M^{(\Delta)}$ is completely determined by Δ and L. This, in general, does not hold for $\mathcal{C}_M^{(\Delta)}$, which also depends on the class of employed quantum states and on the characteristics chosen for encoding the information. The information conveyed by quantum states is retrieved by a quantum receiver, which implements a set of positive operator-valued measures. The goal of the quantum receiver is to determine the state that was transmitted, thus determining the associated symbol. However, since quantum QAM constellations generally do not exhibit GUS, only sub-optimal receivers can be employed to evaluate the SEP.

B. Preliminaries on Hermite Polynomials

As we will see in Sec. III, Hermite polynomials play an important role in the characterization of PAGSs. Here we report some known results on Hermite polynomials that will be used in the following.

For $x \in \mathbb{C}$, the single-variable Hermite polynomial of degree n is

$$H_n(x) = (-1)^n e^{x^2} \frac{d^n}{dx^n} e^{-x^2}\,.$$

For $t, x, y \in \mathbb{C}, |t| < 1$, and $l \in \mathbb{N}$, the bilinear generating function for single-variable Hermite polynomials is [30]

$$\begin{aligned} G(t, x, y; l) &= \sum_{n=0}^{\infty} \frac{t^n}{n!\, 2^n} H_{n+l}(x) H_n(y) \\ &= \frac{G(t, x, y; 0)}{\sqrt{(1-t^2)^l}} H_l\left(\frac{x - yt}{\sqrt{1-t^2}}\right) \end{aligned} \tag{3}$$

where $G(t, x, y; 0)$ is the Mehler's kernel formula given by

$$G(t, x, y; 0) = \frac{e^{(1-t^2)^{-1}\left[2xyt - (x^2+y^2)t^2\right]}}{\sqrt{1-t^2}}\,.$$

III. Pure Photon-Added Gaussian States

This section presents pure PAGSs and derives their Fock representation and inner product.

A. Definition of Pure Photon-Added Gaussian States

Consider a single bosonic mode associated with a Hilbert space $\mathcal{H}$ and satisfying the canonical commutation relation $[\![\boldsymbol{A}, \boldsymbol{A}^\dagger]\!]_- = \boldsymbol{I}_\mathcal{H}$. According to Caves' convention [31], a Gaussian state $|\mu, \zeta\rangle$ is defined as

$$|\mu, \zeta\rangle = \boldsymbol{D}_\mu \boldsymbol{S}_\zeta |0\rangle \tag{4}$$

where $|0\rangle$ is the vacuum state. A k-PAGS is obtained by performing k creation operations on $|\mu, \zeta\rangle$ as [32], [33]

$$|\psi^{(k)}(\mu, \zeta)\rangle = \frac{1}{N^{(k)}(\mu, \zeta)} \left(\boldsymbol{A}^\dagger\right)^k |\mu, \zeta\rangle \tag{5}$$

where $N^{(k)}(\mu, \zeta)$ is the associated normalization constant (photon-addition produces a non-unitary transformation) given by

$$N^{(k)}(\mu, \zeta) = \sqrt{\langle \zeta, \mu | \boldsymbol{A}^k (\boldsymbol{A}^\dagger)^k | \mu, \zeta\rangle}\,. \tag{6}$$

According to Yuen's convention [34], the Gaussian state $|\mu, \zeta\rangle$ defined in (4) can equivalently be written as

$$|\mu, \zeta\rangle = \boldsymbol{S}_\zeta \boldsymbol{D}_{\mu\lambda + \mu^*\nu} |0\rangle \tag{7}$$

where

$$\lambda = \cosh(|\zeta|) \tag{8a}$$

$$\nu = e^{\imath(\theta+\pi)} \sinh(|\zeta|) \tag{8b}$$

generate the linear transformation $\hat{\boldsymbol{A}} = \lambda \boldsymbol{A} + \nu \boldsymbol{A}^\dagger$. Such transformation preserves the canonical commutation relation $[\![\hat{\boldsymbol{A}}, \hat{\boldsymbol{A}}^\dagger]\!]_- = [\![\boldsymbol{A}, \boldsymbol{A}^\dagger]\!]_- = \boldsymbol{I}_\mathcal{H}$. In this paper, we adopt Caves' convention. Notice that (5) is general and can be used to obtain any kind of Gaussian state by setting $k = 0$. For example, by using $k = 0$ and $\zeta = 0$, (5) gives a coherent state.

An important property of Gaussian states is given by their closure under rotational transformations. Indeed, from the Baker-Campbell-Hausdorff formula [35], a rotated Gaussian state $\boldsymbol{R}_\phi \boldsymbol{D}_\mu \boldsymbol{S}_\zeta |0\rangle$ can equivalently be written as

$$\boldsymbol{R}_\phi \boldsymbol{D}_\mu \boldsymbol{S}_\zeta |0\rangle = \boldsymbol{D}_{\mu e^{\imath\phi}} \boldsymbol{S}_{\zeta e^{\imath 2\phi}} |0\rangle\,. \tag{9}$$

Specifically, (9) shows that it is not restrictive to operate with Gaussian states defined as in (4) since any rotated Gaussian state can always be written as a Gaussian state by transforming both displacing and squeezing parameter according to (9).

$$\langle\psi^{(h)}(\xi,\gamma)|\psi^{(k)}(\mu,\zeta)\rangle = \frac{\Lambda^*(\xi,\gamma)\Lambda(\mu,\zeta)}{N^{(h)}(\xi,\gamma)N^{(k)}(\mu,\zeta)\sqrt{\left(2e^{\imath(\theta+\pi)}\tanh(|\zeta|)\right)^{k-h}}} \times\frac{\partial^h}{\partial\rho(\gamma,\zeta)^h}\left[\rho(\gamma,\zeta)^k\, G\big(\rho(\gamma,\zeta),\eta^*(\xi,\gamma),\eta(\mu,\zeta);k-h\big)\right] \tag{14}$$

B. Fock Representation of a Pure PAGS

The Fock representation of pure PAGSs is required for deriving their inner product, which is crucial to analyze the SEP of quantum communication systems employing PAGSs. The Fock representation of a pure PAGS is provided by the following lemma.

Lemma 1 (Fock representation of a pure PAGS): Consider a pure PAGS $|\psi^{(k)}(\mu,\zeta)\rangle\in\mathcal{H}$. Its representation in the Fock space is given by

$$|\psi^{(k)}(\mu,\zeta)\rangle = \frac{1}{N^{(k)}(\mu,\zeta)}\sum_{n=0}^{\infty} c_n^{(k)}(\mu,\zeta)\,|n+k\rangle \tag{10}$$

where

$$c_n^{(k)}(\mu,\zeta) = \frac{\Lambda(\mu,\zeta)}{n!}\sqrt{\frac{(n+k)!\left(e^{\imath(\theta+\pi)}\tanh(|\zeta|)\right)^n}{2^n}} \times H_n\big(\eta(\mu,\zeta)\big) \tag{11}$$

with

$$\Lambda(\mu,\zeta) \triangleq \sqrt{\operatorname{sech}(|\zeta|)} \times\exp\left\{-\frac{1}{2}\left(|\mu|^2+(\mu^*)^2e^{\imath(\theta+\pi)}\tanh(|\zeta|)\right)\right\} \tag{12}$$

$$\eta(\mu,\zeta) \triangleq \frac{\mu+\mu^* e^{\imath(\theta+\pi)}\tanh(|\zeta|)}{\sqrt{2\,e^{\imath(\theta+\pi)}\tanh(|\zeta|)}}\,. \tag{13}$$

Proof: See Appendix A. □

C. Inner Product of Pure PAGSs

In the following, we derive a closed-form expression for the inner product of two pure PAGSs.

Theorem 1 (Inner product of two pure PAGSs): Consider two pure PAGSs $|\psi^{(k)}(\mu,\zeta)\rangle$ and $|\psi^{(h)}(\xi,\gamma)\rangle\in\mathcal{H}$, with, $k,h\in\mathbb{N}$, $k\geqslant h$ without loss of generality, $\mu,\zeta,\xi,\gamma\in\mathbb{C}$, $\zeta=|\zeta|e^{\imath\theta}$, and $\gamma=|\gamma|e^{\imath\varphi}$. The inner product $\langle\psi^{(h)}(\xi,\gamma)|\psi^{(k)}(\mu,\zeta)\rangle$ is given by (14) at the top of the page, where

$$\rho(\gamma,\zeta)\triangleq\sqrt{e^{\imath(\theta-\varphi)}\tanh(|\gamma|)\tanh(|\zeta|)}\,. \tag{15}$$

Proof: See Appendix B. □

Notice that (29c) can be used to obtain the normalization constant $N^{(k)}(\mu,\zeta)$ in (6) by setting $h=k$, $\xi=\mu$, and $\gamma=\zeta$. Therefore, the quantity $\langle\gamma,\xi|\boldsymbol{A}^h\left(\boldsymbol{A}^\dagger\right)^k|\mu,\zeta\rangle$ completely determines $\langle\psi^{(h)}(\xi,\gamma)|\psi^{(k)}(\mu,\zeta)\rangle$. Furthermore, $\langle\gamma,\xi|\boldsymbol{A}^h\left(\boldsymbol{A}^\dagger\right)^k|\mu,\zeta\rangle$ also determines the mean number of photons $\bar{n}_{\mathrm{p}}^{(k)}(\mu,\zeta)$, which is found to be

$$\bar{n}_{\mathrm{p}}^{(k)}(\mu,\zeta) = \left[\frac{N^{(k+1)}(\mu,\zeta)}{N^{(k)}(\mu,\zeta)}\right]^2 - 1\,. \tag{16}$$

IV. Quantum QAM with Pure PAGSs

This section develops the quantum QAM technique with pure PAGSs.[1]

A QAM constellation with pure PAGSs can be constructed by exploiting rotational symmetries exhibited by the geometrical structure of the alphabet of symbols $\mathcal{A}_M^{(\Delta)}$. In the following, we show how to construct arbitrary M-QAM constellations of PAGSs from $M/4$ quaternary PSK sub-constellations.[2] The advantage of this method relies on the fact that PSK constellations exhibit GUS and can be generated by multiple rotations of a reference state. From (1) and (2), the quantum constellation of PAGSs for the M-QAM technique is

$$\mathcal{C}_M^{(\Delta,k)} \triangleq \left\{\,|\psi^{(k)}(a_{i,j},\zeta_{a_{i,j}})\rangle\in\mathcal{H}, a_{i,j}\in\mathcal{A}_M^{(\Delta)}\right\} \tag{17}$$

where $a_{i,j}$ determines both the displacing parameter and the squeezing parameter of $|\psi^{(k)}(a_{i,j},\zeta_{a_{i,j}})\rangle$. Therefore, for a given k, $|\psi^{(k)}(a_{i,j},\zeta_{a_{i,j}})\rangle$ is completely determined by $a_{i,j}$. The geometrical interpretation of (17) can be seen in the phase space, where $|\psi^{(k)}(a_{i,j},\zeta_{a_{i,j}})\rangle$ is represented by an ellipse centered at $a_{i,j}$, with eccentricity and orientation determined by $\zeta_{a_{i,j}}$ (see Fig. 1). In particular, the eccentricity depends on $|\zeta_{a_{i,j}}|$, while the orientation, i.e., the direction of the semi-major axis, is given by $\arg\{\zeta_{a_{i,j}}\}/2$. We then define

$$\mathcal{R}_M^{(\Delta,k)} \triangleq \left\{\,|\psi^{(k)}(a_{i,j},\zeta_{a_{i,j}})\rangle\in\mathcal{C}_M^{(\Delta,k)}, \arg\{a_{i,j}\}\in[0,\pi/2)\right\} \tag{18}$$

as the set of quantum states of the constellation that are located in the first quadrant of the phase space. From (18), the quantum M-QAM constellation can be obtained by considering $\mathcal{R}_M^{(\Delta,k)}$ as the set of reference states associated with $M/4$ quaternary PSK sub-constellations. Notice that the number of reference states is $|\mathcal{R}_M^{(\Delta,k)}|=M/4$, and is given by the number of complex symbols $a_{i,j}$ located into the first quadrant of the complex plane. Therefore, the quaternary PSK sub-constellation generated by the reference state $|\psi^{(k)}(a_{i,j},\zeta_{a_{i,j}})\rangle\in\mathcal{R}_M^{(\Delta,k)}$ is

$$\mathcal{C}_{\mathrm{PSK}}^{(\Delta,k)}\left(\,|\psi^{(k)}(a_{i,j},\zeta_{a_{i,j}})\rangle\,\right) \triangleq \Big\{\boldsymbol{R}_{2\pi m/4}|\psi^{(k)}(a_{i,j},\zeta_{a_{i,j}})\rangle\,, \quad m=0,1,2,3\Big\} \tag{19}$$

where, from (9), it is

$$\boldsymbol{R}_{2\pi m/4}|\psi^{(k)}(a_{i,j},\zeta_{a_{i,j}})\rangle = |\psi^{(k)}(a_{i,j}e^{\imath m\pi/2},\zeta_{a_{i,j}}e^{\imath m\pi})\rangle\,. \tag{20}$$

[1]In the remainder of the paper we consider equiprobable symbols, i.e., $\mathbb{P}\{\mathsf{a}=a_{i,j}\}=1/M$.

[2]Arbitrary M-QAM constellations can be constructed from multiple quaternary PSK constellations.

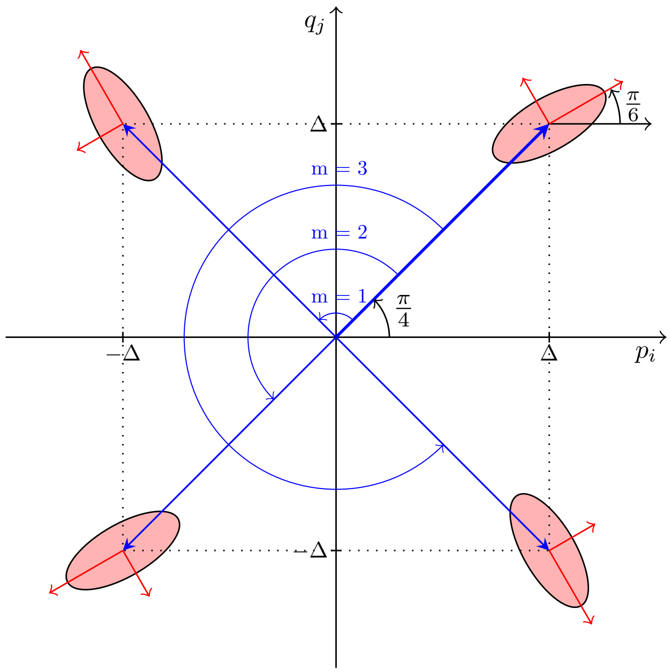

Fig. 1: Representation of the quaternary PSK sub-constellation $\mathcal{C}_{\text{PSK}}^{(\Delta,k)}(|\psi^{(k)}(a_{2,2},\zeta_{a_{2,2}})\rangle)$, where $a_{2,2} = \Delta(1+\imath)$ and $\arg\{\zeta_{a_{2,2}}\} = \pi/3$. The reference state $|\psi^{(k)}(a_{2,2},\zeta_{a_{2,2}})\rangle$ is depicted as the ellipse (contour plot of the associated Wigner function) in the first quadrant and with center determined by the thick blue vector, which represents the displacement $a_{2,2}$ in polar coordinates. The ellipse is tilted of $\arg\{\zeta_{a_{2,2}}\}/2 = \pi/6$. The remaining states are obtained from the anticlockwise rotation of $|\psi^{(k)}(a_{2,2},\zeta_{a_{2,2}})\rangle$ given by (20) with $m = 1, 2, 3$.

Notice that in the phase space, the eccentricity of the ellipses is invariant under rotations. Therefore, states of the same quaternary PSK sub-constellation differ only in the elliptical centers and orientations (see Fig. 1). Finally, from (19) and (20) the M-QAM constellation of PAGSs can be written as

$$\mathcal{C}_M^{(\Delta,k)} = \bigcup_{|\psi^{(k)}(a_{i,j},\zeta_{a_{i,j}})\rangle \in \mathcal{R}_M^{(\Delta,k)}} \mathcal{C}_{\text{PSK}}^{(\Delta,k)}\left(|\psi^{(k)}(a_{i,j},\zeta_{a_{i,j}})\rangle\right) \tag{21}$$

and it is completely determined by $\mathcal{R}_M^{(\Delta,k)}$. The effects of L and Δ on $\mathcal{C}_M^{(\Delta,k)}$ can be appreciated in the phase space. Specifically, L determines the number $M = L^2$ of ellipses (representing quantum states of $\mathcal{C}_M^{(\Delta,k)}$), while Δ impacts on their position and eccentricity, which depend on $a_{i,j}$ and $\zeta_{a_{i,j}}$, respectively. Notice that from the generality of PAGSs and the method for constructing arbitrary quantum M-QAM constellations, (21) can also describe constellations of any kind of pure Gaussian states as a particular case. For example, for $k = 0$ (i.e., no photon-additions) and $\zeta = 0$ (i.e., no squeezing), (21) describes a constellation of coherent states.

V. Performance of Quantum QAM with Pure PAGSs

In this section, we evaluate the performance of quantum QAM communications with pure PAGSs. In particular, we compare the SEP obtained when employing PAGSs with the one given by conventional coherent states.

A. Square Root Measurement Receiver

Classical symbols of the alphabet $\mathcal{A}_M^{(\Delta)}$ are encoded into the corresponding quantum states, elements of the M-QAM constellation $\mathcal{C}_M^{(\Delta,k)}$ sent through a quantum channel.[3] The SEP is related to the probability of the quantum receiver to wrongly discriminate the received quantum states. Recall that quantum QAM constellations generally do not exhibit GUS except for particular cases (e.g., $L = 2$). Therefore, evaluating the SEP requires to employ sub-optimal receivers. In this paper, we evaluate the SEP by using the sub-optimal SRM receiver, which is optimal when constellations exhibit GUS [26]–[28]. For an M-QAM constellation, the SEP P_{e} obtained when employing the SRM receiver is [20]

$$P_{\text{e}} = 1 - \frac{1}{M}\sum_{i=1}^{M}\left[(\boldsymbol{G}^{\frac{1}{2}})_{ii}\right]^2 \tag{22}$$

where $(\boldsymbol{G}^{\frac{1}{2}})_{ij}$ is the element in the i-th row and j-th column in the square root of the Hermitian $M \times M$ Gram matrix $\boldsymbol{G}$, whose elements are the inner products of the quantum states of the quantum M-QAM constellation.

The PAGSs can be obtained by applying, in this order, squeezing and photon-addition operations on initial coherent states generated by a coherent source (e.g., laser). Therefore, the P_{e} in (22) can be evaluated for different values of the mean number of signal photons $\bar{n}_{\text{s}}$ utilized by the coherent source to generate the initial constellation of coherent states. In particular, it is

$$\bar{n}_{\text{s}} = \frac{1}{M}\sum_{i=1}^{L}\sum_{j=1}^{L}\bar{n}_{\text{p}}^{(0)}(a_{i,j},0) \tag{23}$$

$$= \frac{2}{3}(M-1)\Delta^2 \tag{24}$$

where (24) is obtained by using (16) in (23).

B. Performance Evaluation

Fig. 2 shows the P_{e} as a function of $\bar{n}_{\text{s}}$ for 4-QAM ($L = 2$) constellations employing coherent states and PAGSs. The squeezing parameter of the reference PAGS is set to $\zeta_{a_{2,2}} = -0.5\imath$. It can be noticed that when employing PAGSs, the P_{e} decreases with k. This can be attributed to the photon-addition operations that increase the mean number of photons of the initial Gaussian states, thus resulting in a more spaced constellations. Fig. 2 also shows, for each k, the values of $\bar{n}_{\text{s}}$ for which PAGSs perform better than coherent states.

A similar behavior can be observed from Fig. 3, which depicts the P_{e} as a function of $\bar{n}_{\text{s}}$ for 16-QAM ($L = 4$) constellations employing coherent states and PAGSs. In this case, the squeezing parameter of the reference PAGSs is given by the associated symbol $a_{i,j}$. Note that in this scenario, the beneficial effects of the photon-addition operation are more

[3] In the following, an ideal quantum channel is considered.

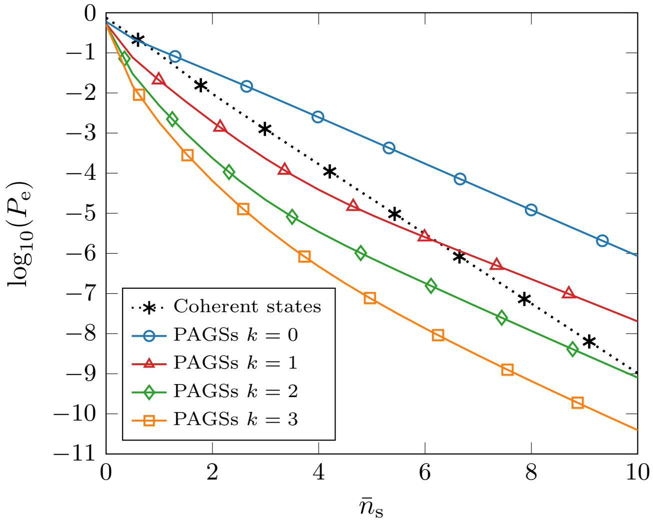

Fig. 2: P_{e} for 4-QAM constellations of (a) coherent states (black dotted line); and (b) PAGSs with $k = 0$ (solid blue line), $k = 1$ (solid red line), $k = 2$ (solid green line), and $k = 3$ (solid orange line). For each k, the squeezing parameter of the reference PAGS $|\psi^{(k)}(a_{i,j}, \zeta_{a_{i,j}})\rangle \in \mathcal{R}_4^{(\Delta,k)}$ is set to $\zeta_{a_{2,2}} = -0.5\imath$.

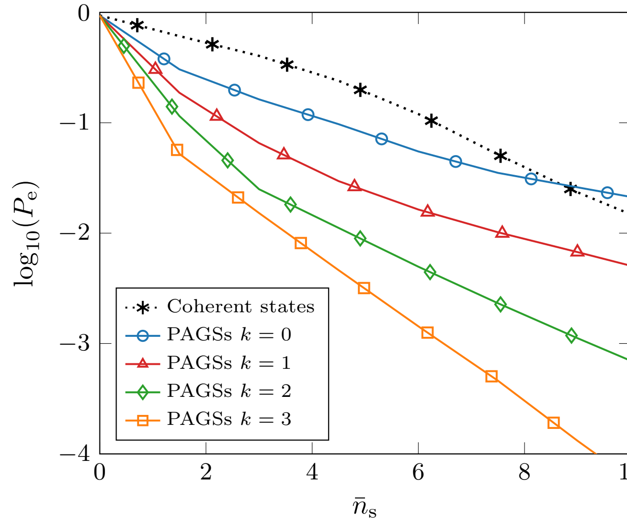

Fig. 3: P_{e} for 16-QAM constellations of (a) coherent states (black dotted line); and (b) PAGSs with $k = 0$ (solid blue line), $k = 1$ (solid red line), $k = 2$ (solid green line), and $k = 3$ (solid orange line). For each k, the squeezing parameter of the reference PAGSs $|\psi^{(k)}(a_{i,j}, \zeta_{a_{i,j}})\rangle \in \mathcal{R}_{16}^{(\Delta,k)}$ is set to $\zeta_{a_{i,j}} = a_{i,j}$.

relevant compared to the ones shown in Fig. 2. Indeed, except for high values of $\bar{n}_{\mathrm{s}}$ with $k = 0$, PAGSs always provide a performance gain with respect to coherent states.

Further important considerations can be made for Fig. 2 and Fig. 3. In particular, notice that for the same $\bar{n}_{\mathrm{s}}$, as for classical systems, the P_{e} increases with M. This can be attributed to the fact that when the same amount of energy is employed to produce higher dimensional constellations, the scale factor Δ (i.e., the distance between the states of the constellation) is reduced. Fig. 2 and Fig. 3 also show the operating regimes in which PAGSs perform better than coherent states, thus opening the possibility of engineering and optimizing the quantum constellations. Finally, notice that the 4-QAM discussed in Fig. 2 is equivalent to a quaternary PSK, thus exhibiting GUS. Therefore, the P_{e} shown in Fig. 2 is the minimum SEP.

VI. Conclusion

This paper explored the use of pure non-Gaussian PAGSs for quantum QAM communications. In particular, after characterizing pure PAGSs in the Fock space and providing a closed-form expression of their inner product, it is shown how to construct arbitrary QAM constellations of PAGSs from multiple PSK sub-constellations. Finally, the performance of QAM with PAGSs is evaluated and compared with the one provided by conventional coherent states. The mathematical description of QAM constellations of PAGSs is general and can also be used to describe QAM constellations of pure Gaussian states as a particular case. Performance evaluation shows that PAGSs can offer a performance gain with respect to conventional coherent states. The findings of this paper provide useful insights for developing quantum communication systems with non-Gaussian states and multilevel modulations.

Appendix A
Proof of Lemma 1

We recall the well-known relation for $\boldsymbol{A}^\dagger$

$$(\boldsymbol{A}^\dagger)^k |n\rangle = \sqrt{\frac{(n+k)!}{n!}}\, |n+k\rangle \,. \tag{25}$$

Consider a pure PAGS $|\psi^{(k)}(\mu,\zeta)\rangle \in \mathcal{H}$ obtained from the Gaussian state $|\mu,\zeta\rangle$ defined as in (4). By expanding $|\mu,\zeta\rangle$ in the Fock basis and by using (25), (5) can be written as

$$|\psi^{(k)}(\mu,\zeta)\rangle = \frac{1}{N^{(k)}(\mu,\zeta)} \sum_{n=0}^{\infty} \langle n|\zeta,\mu\rangle \sqrt{\frac{(n+k)!}{n!}}\, |n+k\rangle \tag{26}$$

$$= \frac{1}{N^{(k)}(\mu,\zeta)} \sum_{n=0}^{\infty} \langle n|\, \boldsymbol{S}_\zeta \boldsymbol{D}_{\mu\lambda+\mu^*\nu} |0\rangle \times \sqrt{\frac{(n+k)!}{n!}}\, |n+k\rangle \tag{27}$$

where (27) is obtained by using (7) in (26). Finally, (11) follows after using [34, Eq. (3.23)] together with (8), (12), and (13) in (27).

Appendix B
Proof of Theorem 1

Consider two pure PAGSs $|\psi^{(k)}(\mu,\zeta)\rangle\,, |\psi^{(h)}(\xi,\gamma)\rangle \in \mathcal{H}$, where, without loss of generality, $k \geqslant h$. By using (5), the inner product of the two PAGSs can be written as

$$\langle\psi^{(h)}(\xi,\gamma)|\psi^{(k)}(\mu,\zeta)\rangle = \frac{\langle\gamma,\xi|\boldsymbol{A}^h \left(\boldsymbol{A}^\dagger\right)^k|\mu,\zeta\rangle}{N^{(h)}(\xi,\gamma)N^{(k)}(\mu,\zeta)} \,. \tag{28}$$

From (10) and (11), $\langle\gamma,\xi|\boldsymbol{A}^h \left(\boldsymbol{A}^\dagger\right)^k|\mu,\zeta\rangle$ can be written as in (29a) at the top of the next page. By denoting $j = k - h \geqslant 0$

$$\langle\gamma,\xi|\boldsymbol{A}^h\big(\boldsymbol{A}^\dagger\big)^k|\mu,\zeta\rangle = \sum_{m=0}^{\infty}\sum_{n=0}^{\infty}\frac{\Lambda^*(\xi,\gamma)\Lambda(\mu,\zeta)}{m!\,n!}\sqrt{\frac{(m+h)!\big(e^{-\imath(\varphi+\pi)}\tanh(|\gamma|)\big)^m}{2^m}}\sqrt{\frac{(n+k)!\big(e^{\imath(\theta+\pi)}\tanh(|\zeta|)\big)^n}{2^n}} \times H_m\big(\eta^*(\xi,\gamma)\big)H_n\big(\eta(\mu,\zeta)\big)\,\langle m+h|n+k\rangle \tag{29a}$$

$$= \frac{\Lambda^*(\xi,\gamma)\Lambda(\mu,\zeta)}{\sqrt{\big(2e^{\imath(\theta+\pi)}\tanh(|\zeta|)\big)^{k-h}}}\sum_{n=0}^{\infty}\frac{(n+k)!}{(n+k-h)!\,n!}\frac{\rho(\gamma,\zeta)^{n+k-h}}{2^n}H_{n+k-h}\big(\eta^*(\xi,\gamma)\big)H_n\big(\eta(\mu,\zeta)\big) \tag{29b}$$

$$= \frac{\Lambda^*(\xi,\gamma)\Lambda(\mu,\zeta)}{\sqrt{\big(2e^{\imath(\theta+\pi)}\tanh(|\zeta|)\big)^{k-h}}}\frac{\partial^h}{\partial\rho(\gamma,\zeta)^h}\left[\rho(\gamma,\zeta)^k\sum_{n=0}^{\infty}\frac{\rho(\gamma,\zeta)^n}{n!\,2^n}H_{n+k-h}\big(\eta^*(\xi,\gamma)\big)H_n\big(\eta(\mu,\zeta)\big)\right] \tag{29c}$$

and $p=m-j$ in (29a), and exploiting (15) together with the orthonormality of the Fock basis, we obtain (29b). Now, by noticing that $(\partial/\partial x)^p x^m = (m!/(m-p)!)x^{m-p}$, (29b) can be written as (29c). Finally, by using (29c) and (3) in (28), and noticing that $|\rho(\gamma,\zeta)|<1, \forall\,\gamma,\zeta\in\mathbb{C}$, we obtain (14).

Acknowledgment

The fundamental research described in this paper was supported, in part, by the Ministero dell'Università e della Ricerca under Grant 2022JES5S2 and by the Office of Naval Research under Grant N00014-19-1-2724.

References

[1] C. Helstrom, J. Liu, and J. Gordon, "Quantum-mechanical communication theory," *Proc. IEEE*, vol. 58, no. 10, pp. 1578–1598, Oct. 1970.

[2] J. E. Mazo and J. Salz, "On optical data communication via direct detection of light pulses," *Bell Syst. Tech. J.*, vol. 55, no. 3, pp. 347–369, Mar. 1976.

[3] L. Mandel, "Ideal light source for an optical communication channel," *J. Opt. Soc. Amer.*, vol. 66, no. 9, pp. 968–970, Sep. 1976.

[4] H. Yuen and J. Shapiro, "Optical communication with two-photon coherent states–Part I: Quantum-state propagation and quantum-noise," *IEEE Trans. Inf. Theory*, vol. 24, no. 6, pp. 657–668, Nov. 1978.

[5] R. Slusher and B. Yurke, "Squeezed light for coherent communications," *J. Lightw. Technol.*, vol. 8, no. 3, pp. 466–477, Mar. 1990.

[6] X.-B. Wang, T. Hiroshima, A. Tomita, and M. Hayashi, "Quantum information with Gaussian states," *Phys. Rep.*, vol. 448, no. 1, pp. 1–111, Aug. 2007.

[7] G. Cariolaro, *Quantum Communications*. Switzerland: Springer International Publishing, 2015.

[8] C. W. Helstrom, "Quantum detection and estimation theory," *J. Statist. Phys.*, vol. 1, no. 2, pp. 231–252, Jun. 1969.

[9] A. Holevo, "Statistical decision theory for quantum systems," *J. Multivariate Anal.*, vol. 3, no. 4, pp. 337–394, Dec. 1973.

[10] S. Guerrini, M. Z. Win, M. Chiani, and A. Conti, "Quantum discrimination of noisy photon-added coherent states," *IEEE J. Sel. Areas Inf. Theory*, vol. 1, no. 2, pp. 469–479, Aug. 2020.

[11] A. Giani, M. Z. Win, and A. Conti, "Quantum discrimination of noisy photon-subtracted squeezed states," in *Proc. IEEE Global Telecomm. Conf.*, Rio de Janeiro, Brazil, Dec. 2022, pp. 5826–5831.

[12] S. Marano and M. Z. Win, "Distributing quantum states with finite lifetime," *Phys. Rev. A*, vol. 107, no. 5, p. 052413, May 2023.

[13] H. Yuen, R. Kennedy, and M. Lax, "Optimum testing of multiple hypotheses in quantum detection theory," *IEEE Trans. Inf. Theory*, vol. 21, no. 2, pp. 125–134, Mar. 1975.

[14] A. Waseda *et al.*, "Numerical evaluation of PPM for deep-space links," *J. Opt. Commun. Netw.*, vol. 3, no. 6, pp. 514–521, May 2011.

[15] G. Cariolaro and G. Pierobon, "Theory of quantum pulse position modulation and related numerical problems," *IEEE Trans. Commun.*, vol. 58, no. 4, pp. 1213–1222, Mar. 2010.

[16] G. Cariolaro, R. Corvaja, and G. Pierobon, "Gaussian states and geometrically uniform symmetry," *Phys. Rev. A*, vol. 90, no. 4, p. 042309, Oct. 2014.

[17] F. E. Becerra *et al.*, "M-ary-state phase-shift-keying discrimination below the homodyne limit," *Phys. Rev. A*, vol. 84, no. 6, p. 062324, Dec. 2011.

[18] G. Chesi, S. Olivares, and M. G. A. Paris, "Squeezing-enhanced phase-shift-keyed binary communication in noisy channels," *Phys. Rev. A*, vol. 97, no. 3, p. 032315, Mar. 2018.

[19] J. S. Sidhu, S. Izumi, J. S. Neergaard-Nielsen, C. Lupo, and U. L. Andersen, "Quantum receiver for phase-shift keying at the single-photon level," *PRX Quantum*, vol. 2, no. 1, p. 010332, Feb. 2021.

[20] K. Kato, M. Osaki, M. Sasaki, and O. Hirota, "Quantum detection and mutual information for QAM and PSK signals," *IEEE Trans. Commun*, vol. 47, no. 2, pp. 248–254, Feb. 1999.

[21] G. Cariolaro and G. Pierobon, "Performance of quantum data transmission systems in the presence of thermal noise," *IEEE Trans. Commun.*, vol. 58, no. 2, pp. 623–630, Feb. 2010.

[22] T. Chen, K. Li, Y. Zuo, and B. Zhu, "Hybrid quantum receiver for quadrature amplitude modulation coherent-state discrimination beating the classical limit," *Appl. Opt.*, vol. 57, no. 4, pp. 817–822, Feb. 2018.

[23] C. Cui *et al.*, "Quantum receiver enhanced by adaptive learning," *Light Sci. Appl.*, vol. 11, no. 1, p. 344, Dec. 2022.

[24] S. Guerrini, M. Chiani, M. Z. Win, and A. Conti, "Quantum pulse position modulation with photon-added coherent states," in *Proc. IEEE Workshop on Quantum Commun. and Inf. Technol. (QCIT), Global Telecomm. Conf.*, Waikoloa, HI, Dec. 2019, pp. 1–5.

[25] S. Guerrini, M. Chiani, M. Z. Win, and A. Conti, "Quantum pulse position modulation with photon-added squeezed states," in *Proc. IEEE Workshop on Quantum Commun. and Inf. Technol. (QCIT), Global Telecomm. Conf.*, Taipei, Taiwan, Dec. 2020, pp. 1–5.

[26] Y. Eldar and G. Forney, "On quantum detection and the square-root measurement," *IEEE Trans. Inf. Theory*, vol. 47, no. 3, pp. 858–872, Mar. 2001.

[27] Y. Eldar, A. Megretski, and G. Verghese, "Optimal detection of symmetric mixed quantum states," *IEEE Trans. Inf. Theory*, vol. 50, no. 6, pp. 1198–1207, Jun. 2004.

[28] P. Hausladen and W. K. Wootters, "A 'Pretty Good' measurement for distinguishing quantum states," *J. Modern Opt.*, vol. 41, no. 12, pp. 2385–2390, 1994.

[29] A. Assalini, G. Cariolaro, and G. Pierobon, "Efficient optimal minimum error discrimination of symmetric quantum states," *Phys. Rev. A*, vol. 81, no. 1, p. 012315, Jan. 2010.

[30] G. Dattoli, A. Torre, and M. Carpanese, "Operational rules and arbitrary order Hermite generating functions," *J. Math. Anal. Appl.*, vol. 227, no. 1, pp. 98–111, Nov. 1998.

[31] C. M. Caves, "Quantum-mechanical noise in an interferometer," *Phys. Rev. D*, vol. 23, no. 8, pp. 1693–1708, Apr. 1981.

[32] S. Guerrini, M. Z. Win, and A. Conti, "Photon-varied quantum states: Unified characterization," *Phys. Rev. A*, vol. 108, no. 2, p. 022425, Aug. 2023.

[33] A. Giani, M. Z. Win, and A. Conti, "Source engineering for quantum key distribution with noisy photon-added squeezed states," in *Proc. IEEE Int. Conf. Commun.*, Rome, Italy, May 2023, to appear.

[34] H. P. Yuen, "Two-photon coherent states of the radiation field," *Phys. Rev. A*, vol. 13, no. 6, pp. 2226–2243, Jun. 1976.

[35] B. L. Schumaker, "Quantum mechanical pure states with Gaussian wave functions," *Phys. Rep.*, vol. 135, no. 6, pp. 317–408, Apr. 1986.